Design of Orthonormal and Overcomplete Wavelet Transforms Based on Rational Sampling Factors

İlker Bayram and Ivan W. Selesnick

Polytechnic University, Brooklyn, NY, 11201, USA

ABSTRACT

Most wavelet transforms used in practice are based on integer sampling factors. Wavelet transforms based on rational sampling factors offer in principle the potential for time-scale signal representations having a finer frequency resolution. Previous work on rational wavelet transforms and filter banks includes filter design methods and frequency domain implementations. We present several specific examples of Daubechies-type filters for a discrete orthonormal rational wavelet transform (FIR filters having a maximum number of vanishing moments) obtained using Gröbner bases. We also present the design of overcomplete rational wavelet transforms (tight frames) with FIR filters obtained using polynomial matrix spectral factorization.

Keywords: Rational filter banks, rational wavelets, frames, overcomplete filter banks.

1. INTRODUCTION

In this paper we discuss the design of orthonormal and overcomplete rational discrete wavelet transforms (DWTs) based on the critically-sampled filter bank (FB) illustrated in Fig. 1 and on the overcomplete FB illustrated in Fig. 8. The frequency decomposition typical of the dyadic DWT is illustrated in the top panel of Fig. 2. Using different filters for the dyadic DWT yields different frequency responses but does not alter the Q-factor of the frequency decomposition. If a different Q-factor is desired,[4,6,9,13,14,27] the rational FB in Fig. 1, can be used. The frequency decomposition typical of an orthonormal rational (2/3) DWT, based on the FB in Fig. 1 is illustrated in the center panel of Fig. 2. In this paper we also develop an overcomplete rational (2/3) DWT, the frequency decomposition of which, is illustrated in the bottom panel of Fig. 2. The overcomplete DWT constitutes a 'tight frame', as the synthesis filters are obtained by time-reversing the analysis filters. For many applications, performance can be enhanced by using a frame (a data-expansive transform) in place of a critically-sampled transform.[18] In this case, using tight frames, we are able to choose the low-pass filter more freely, as compared to the orthonormal case. This freedom of choice allows us to eliminate the undesirable side lobes apparent in the center panel of Fig. 2. In addition, the rational wavelet frame is approximately shift invariant. For convenience of notation, we consider the case (2/3) shown in Fig. 1 but the results can be generalized to other sampling factors.

As is well-known, dyadic orthonormal 2-band DWTs (or in general, regular M-band DWTs) with vanishing moments can be designed by performing spectral factorization on a corresponding half-band (M^{th} band for M-band DWTs[30]) autocorrelation sequence, where closed-form expressions for the autocorrelation sequence are available. However, this method is not applicable to rational FBs, because in this case, the PR conditions can not be expressed solely in terms of an autocorrelation sequence. In this paper we present some minimal-length filters designed using Gröbner basis methods (see Ref. 24 for a background on these methods, Ref. 11 for Gröbner bases in general, and Refs. 1, 7, 20, 25, 26, 28, 32, 33 for rational FB design). Using these methods, we are able to compute the shortest filters yielding orthonormal rational FBs with a number of vanishing moments. However, Gröbner basis methods are computationally expensive, and only a few examples can be obtained.

Author information: Email: ibayra01@utopia.poly.edu, selesi@poly.edu, Web: http://utopia.poly.edu/~ibayra01, http://taco.poly.edu/selesi/, Tel: (718) 260-3416.

Wavelet Applications in Industrial Processing V
Proceedings of SPIE Volume 6763
September 11-12, 2007
Boston, USA

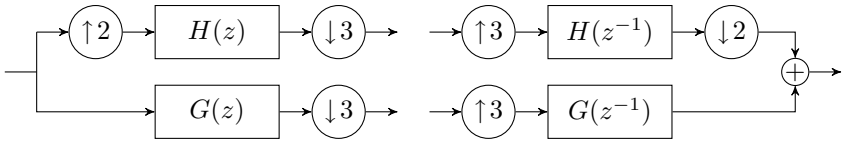

Figure 1. A rational filter bank.

In the second part of this paper, we consider the design of tight wavelet frames based on a rational sampling factor (2/3). Like the double-density DWT,[29] such a frame samples the time-frequency plane more densely than a critically-sampled orthonormal wavelet transform, and can be approximately shift-invariant. Moreover, for frames the restrictions on the low-pass filters can be greatly reduced; it turns out that the design of rational tight frames with polynomial approximation properties can be carried out more easily than the design of rational orthonormal bases. We demonstrate the design of rational tight frames using 'polynomial matrix spectral factorization'. Of the many algorithms to perform matrix spectral factorization,[34] also referred to as the matrix-valued Riesz lemma,[10,17] we used the algorithm described in Ref. 21 because it most closely parallels the polynomial root finding approach for the spectral factorization of univariate polynomials[23] and likewise can provide non-mimimum-phase factorizations. A concise survey of methods and references for matrix spectral factorization are given in Ref. 22 (also see Ref. 16 for 2×2 factorization where each factor is itself symmetric).

A final point should be mentioned regarding the multiresolution analysis (MRA) framework. An MRA with a rational dilation factor was defined by Auscher,[2] sharing the properties of an MRA with an integer

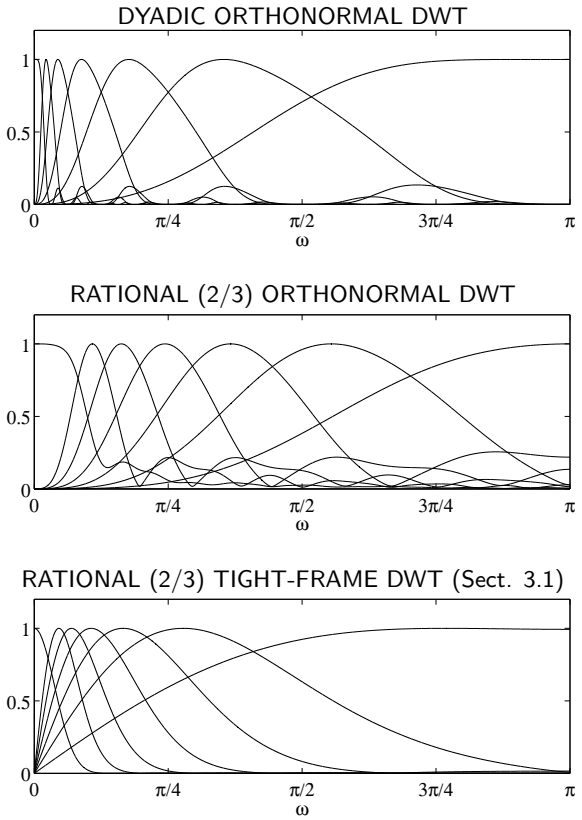

Figure 2. Typical frequency decompositions performed by a dyadic orthonormal DWT, a rational (2/3) orthonormal DWT (Fig. 1), and a rational (2/3) tight-frame DWT (Fig. 8).

dilation factor. Moreover, a fast algorithm to analyze the approximation coefficients into the detail and coarse level approximation coefficients (and synthesize back), like the DWT was derived (and shown to be equivalent to a rational FB) by Baussard et al.[3] However, an MRA with rational dilation factor does not allow compactly supported bases, in contrast to the integer dilation factor case,[2] and does not allow FIR filters in the analysis and synthesis FBs.[5,19] Nevertheless, Blu shows that, like the dyadic case, the basis functions associated with an iterated rational FIR FB can be made smooth with compact support.[5] Although these functions do not satisfy the shift-invariance property required by an MRA, nor are related to an MRA as defined in Ref. 2 (see Ref. 12, section 10.4 for related discussion), the iterated rational filter bank does generate a basis (or frame) for $l_2(\mathbb{Z})$ because it is an invertible discrete transform. We call the basis (frame) a wavelet basis (frame) as it is constructed/implemented via an iterated low-pass/high-pass frequency decomposition. We use the term 'DWT' here in this sense — an iterated low-pass/high-pass frequency decomposition, iterated on the lowpass branch.

2. ORTHONORMAL RATIONAL FILTER BANKS

In this section, we consider orthonormal rational filter banks and their design using Gröbner basis methods. We first derive the perfect reconstruction conditions for the FB in Fig. 1, provide minimal-length solutions for some special cases, and discuss their properties.

Referring to Fig. 3, we have

$$\hat{X}(z) = X(z^2)\, H(z), \tag{1}$$

where $X(z) = \sum_n x(n)\, z^{-n}$, etc. Then, defining $W := e^{j2\pi/3}$,

$$\tilde{X}(z) = \frac{1}{3}\left[\hat{X}(z) + \hat{X}(zW) + \hat{X}(zW^2)\right] \tag{2}$$

$$= \frac{1}{3}\left[X(z^2)\, H(z) + X(z^2W^2)\, H(zW) + X(z^2W)\, H(zW^2)\right], \tag{3}$$

and therefore,

$$\begin{aligned}
Y_1(z) &= \frac{1}{2}\left[\tilde{X}(z^{1/2})H(z^{-1/2}) + \tilde{X}(-z^{1/2})H(-z^{-1/2})\right] \\
&= \frac{1}{6}\left[X(z)H(z^{1/2}) + X(zW^2)H(z^{1/2}W) + X(zW)H(z^{1/2}W^2)\right] H(z^{-1/2}) \\
&\quad + \frac{1}{6}\left[X(z)H(-z^{1/2}) + X(zW^2)H(-z^{1/2}W) + X(zW)H(-z^{1/2}W^2)\right] H(-z^{-1/2}) \\
&= \frac{1}{6}\left[H(z^{1/2})H(z^{-1/2}) + H(-z^{1/2})H(-z^{-1/2})\right] X(z) \\
&\quad + \frac{1}{6}\left[H(z^{1/2}W)H(z^{-1/2}) + H(-z^{1/2}W)H(-z^{-1/2})\right] X(zW^2) \\
&\quad + \frac{1}{6}\left[H(z^{1/2}W^2)H(z^{-1/2}) + H(-z^{1/2}W^2)H(-z^{-1/2})\right] X(zW).
\end{aligned} \tag{4}$$

Similarly,

$$Y_2(z) = \frac{1}{3}\left[G(z)G(z^{-1})X(z) + G(zW)G(z^{-1})X(zW) + G(zW^2)G(z^{-1})X(zW^2)\right]. \tag{5}$$

So that the perfect reconstruction equations are (replacing z by z^2):

$$\frac{1}{6}\left[H(z)\, H(z^{-1}) + H(-z)\, H(-z^{-1})\right] + \frac{1}{3}\, G(z^2)\, G(z^{-2}) = 1, \tag{6}$$

$$\frac{1}{6}\left[H(zW^2)\, H(z^{-1}) + H(-zW^2)\, H(-z^{-1})\right] + \frac{1}{3}\, G(z^2W)\, G(z^{-2}) = 0, \tag{7}$$

$$\frac{1}{6}\left[H(zW)\, H(z^{-1}) + H(-zW)\, H(-z^{-1})\right] + \frac{1}{3}\, G(z^2W^2)\, G(z^{-2}) = 0. \tag{8}$$

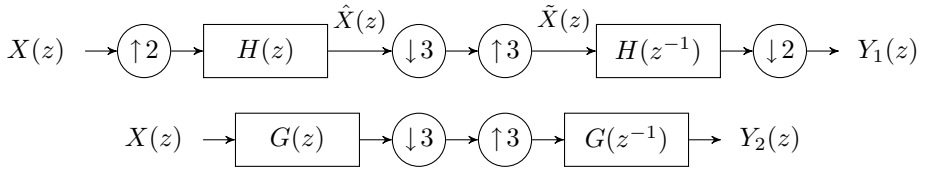

Figure 3. The low-pass and high-pass branches of a rational filter bank.

Modulating this set of equations by W and W^2, we can write,

$$\begin{pmatrix} H(z) & H(-z) & \sqrt{2}\,G(z^2) \\ H(zW^2) & H(-zW^2) & \sqrt{2}\,G(z^2W) \\ H(zW) & H(-zW) & \sqrt{2}\,G(z^2W^2) \end{pmatrix} \begin{pmatrix} H(z^{-1}) & H(z^{-1}W) & H(z^{-1}W^2) \\ H(-z^{-1}) & H(-z^{-1}W) & H(-z^{-1}W^2) \\ \sqrt{2}\,G(z^{-2}) & \sqrt{2}\,G(z^{-2}W^2) & \sqrt{2}\,G(z^{-2}W) \end{pmatrix} = 6\,I \tag{9}$$

Switching the two matrices in (9), we obtain,

$$\begin{pmatrix} H(z^{-1}) & H(z^{-1}W) & H(z^{-1}W^2) \\ H(-z^{-1}) & H(-z^{-1}W) & H(-z^{-1}W^2) \\ \sqrt{2}\,G(z^{-2}) & \sqrt{2}\,G(z^{-2}W^2) & \sqrt{2}\,G(z^{-2}W) \end{pmatrix} \begin{pmatrix} H(z) & H(-z) & \sqrt{2}\,G(z^2) \\ H(zW^2) & H(-zW^2) & \sqrt{2}\,G(z^2W) \\ H(zW) & H(-zW) & \sqrt{2}\,G(z^2W^2) \end{pmatrix} = 6\,I \tag{10}$$

Due primarily to the existence of the complex terms containing W, we will not use (10) for Gröbner basis computations. However, (10) will be useful for investigating properties of orthonormal rational filter banks.

2.1 Equations for Gröbner basis Computation

In this subsection, we replace (6), (7), (8) by equivalent equations, which are more suitable for Gröbner basis computation. The new set of equations can be extended to more general sampling factors straightforwardly.

From Fig. 4, it is seen that the polyphase components of $H(z)$, defined through

$$H(z) = H_0(z^2) + z^{-3}\,H_1(z^2), \tag{11}$$

form two channels of a 3-channel FB. (Note that this is different from the usual definition of $H_1(z)$ by a delay of 2 samples.) It follows that,

$$[\downarrow 3]\ \left\{H_0(z)\,H_0(z^{-1})\right\} = 1, \tag{12}$$

$$[\downarrow 3]\ \left\{H_1(z)\,H_1(z^{-1})\right\} = 1, \tag{13}$$

$$[\downarrow 3]\ \left\{H_0(z)\,H_1(z^{-1})\right\} = 0. \tag{14}$$

Noting that,

$$H_0(z^2)\,H(z^{-1}) = H_0(z^2)[H_0(z^{-2}) + z^3 H_1(z^{-2})] = H_0(z^2)\,H_0(z^{-2}) + z^3[H_0(z^2)\,H_1(z^{-2})],$$

we have, by (12) and (14),

$$[\downarrow 3]\ \left\{H_0(z^2)\,H(z^{-1})\right\} = 1. \tag{15}$$

Appending the unit energy constraint for the second band as well,

$$\sum h_1^2(n) = 1 \tag{16}$$

it is seen that, (15), (16) imply (12), (13), (14). Alternatively, for the sake of generalizability, we can consider instead of (16),

$$[\downarrow 3]\ \left\{z^{-3}H_1(z^2)\,H(z^{-1})\right\} = 1. \tag{17}$$

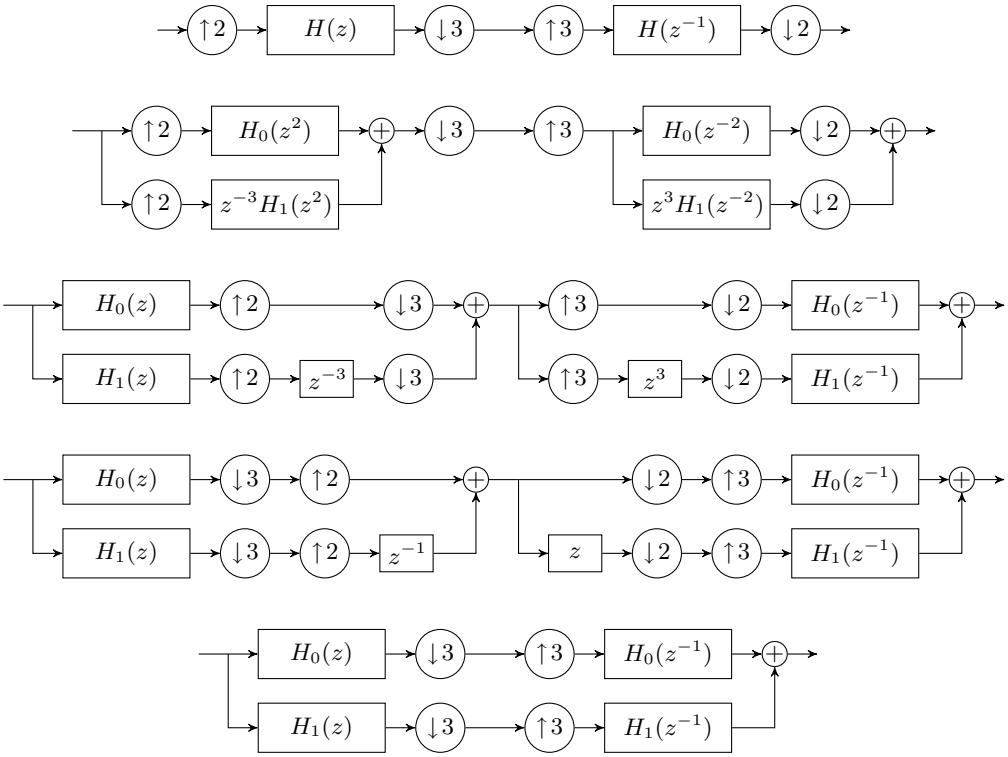

Figure 4. The transformation of the low-pass branch of a rational (2/3) filter bank into two channels of a three-channel filter bank. The polyphase components of $H(z)$ are defined through (11).

which can be derived similar to (15).

Now we can show the equivalence of (15), (17) to (10). Rewriting (15),

$$[\downarrow 3]\ \left\{H_0(z^2)\,H(z^{-1})\right\} = [\downarrow 3]\ \left\{\frac{1}{2}[H(z)+H(-z)]\,H(z^{-1})\right\} = 1. \tag{18}$$

Rewriting (17),

$$[\downarrow 3]\ \left\{z^{-3}H_1(z^2)\,H(z^{-1})\right\} = [\downarrow 3]\ \left\{\frac{1}{2}[H(z)-H(-z)]\,H(z^{-1})\right\} = 1. \tag{19}$$

Adding and subtracting these two equations, we get respectively,

$$[\downarrow 3]\ \left\{H(z)\,H(z^{-1})\right\} = 2 \tag{20}$$

$$[\downarrow 3]\ \left\{H(-z)\,H(z^{-1})\right\} = 0. \tag{21}$$

But these are exactly the two equations obtained from (10) (row1 $\times$ column1 $= 1$, row1 $\times$ column2 $= 0$.)

Summarizing, for Gröbner basis calculation, the equations used are (15), (16) and the vanishing moment conditions (26) (for K vanishing moments) which can be expressed equivalently as:

$$\text{rem}\left(H(z), (z^2+z+1)^K\right) = 0. \tag{22}$$

where 'rem' denotes the remainder after polynomial division.

For a length 11 filter with 2 vanishing moments, the equations are as follows:

Table 1. Minimal-length filters for orthonormal (2/3) rational filter bank having K vanishing moments; $K = 1, 2, 3$. The low-pass filter is given by $H(z) = Q(z)[(1 + z + z^2)(1 + z)]^K$. The filters are illustrated in Fig. 5.

	$K=1$		$K=2$		$K=3$	
n	$q(n)$	$g(n)$	$q(n)$	$g(n)$	$q(n)$	$g(n)$
0	0.258819045102	0	-0.010386345297	0.002349103722	0.000507538600	0.056703525040
1	0.298858490722	0	0.041545381190	-0.051342646308	-0.003045231599	-0.002448165403
2	-0.149429245361	-0.577350269189	0.143916009556	-0.214529595761	0.009113781904	-0.435710813865
3	0	0.788675134594	-0.142711551606	0.731437203991	-0.033792694376	0.754817090467
4	0	-0.211324865405	0.035677887901	-0.625660554077	0.117029410284	-0.476122043329
5			0	0.157746488433	-0.125281778857	0.102436385629
6					0.056171045203	0.000627178746
7					-0.009361840867	-0.000386952702
8					0	0.000083795418

```
\\Orthonormality equations
h(0)^2+h(2)^2+h(4)^2+h(6)^2+h(8)^2+h(10)^2-1=0
h(1)^2+h(3)^2+h(5)^2+h(7)^2+h(9)^2-1=0
h(0)*h(3)+h(2)*h(5)+h(4)*h(7)+h(6)*h(9)=0
h(0)*h(6)+h(2)*h(8)+h(4)*h(10)=0
h(0)*h(9)=0
h(1)*h(4)+h(3)*h(6)+h(5)*h(8)+h(7)*h(10)=0 h(1)*h(7)+h(3)*h(9)=0
h(1)*h(10)=0

\\Vanishing Moment Equations
h(0)-h(4)+2*h(5)-h(6)-2*h(7)+4*h(8)-2*h(9)-3*h(10)=0
h(1)-2*h(4)+3*h(5)-5*h(7)+6*h(8)-8*h(10)=0
h(2)-3*h(4)+4*h(5)-6*h(7)+7*h(8)-9*h(10)=0
h(3)-2*h(4)+h(5)+2*h(6)-4*h(7)+2*h(8)+3*h(9)-6*h(10)=0
```

Following Ref. 24, we can replace the first two of the orthonormality equations, with the following two equations:

```
h(0)+h(2)+h(4)+h(6)+h(8)+h(10)-1=0
h(1)+h(3)+h(5)+h(7)+h(9)-1=0
```

This normalization reduces the number of solutions provided by the Gröbner bases and thereby reduces the computational burden. (The quadratic energy normalization is replaced here by a linear normalization.) The solutions found using this updated set of equations must be normalized taking into account that $H(1) = \sqrt{6}$.

Minimal-length low-pass filters $H(z)$ and high-pass filters $G(z)$ with 1, 2 and 3 vanishing moments are obtained by obtaining Gröbner bases using the software, SINGULAR.[15] In each case, several solutions exist to the nonlinear design equations (some solutions have poor frequency responses). The best solutions are tabulated in Table 1 and illustrated in Fig. 5.

2.2 Zeros of $H(z)$ and $G(z)$ at $z = -1$ and $z = 1$

In the implementation of a rational DWT, we iterate the low-pass filter in Fig. 1. This is equivalent to a system comprised of an upsampler followed by a filter and a downsampler as shown in Fig. 6, where $H^{(j)}(z)$ can be determined using noble identities[31]

$$H^{(j)}(z) = \prod_{k=0}^{j-1} H(z^{2^{j-1-k}\,3^k}). \tag{23}$$

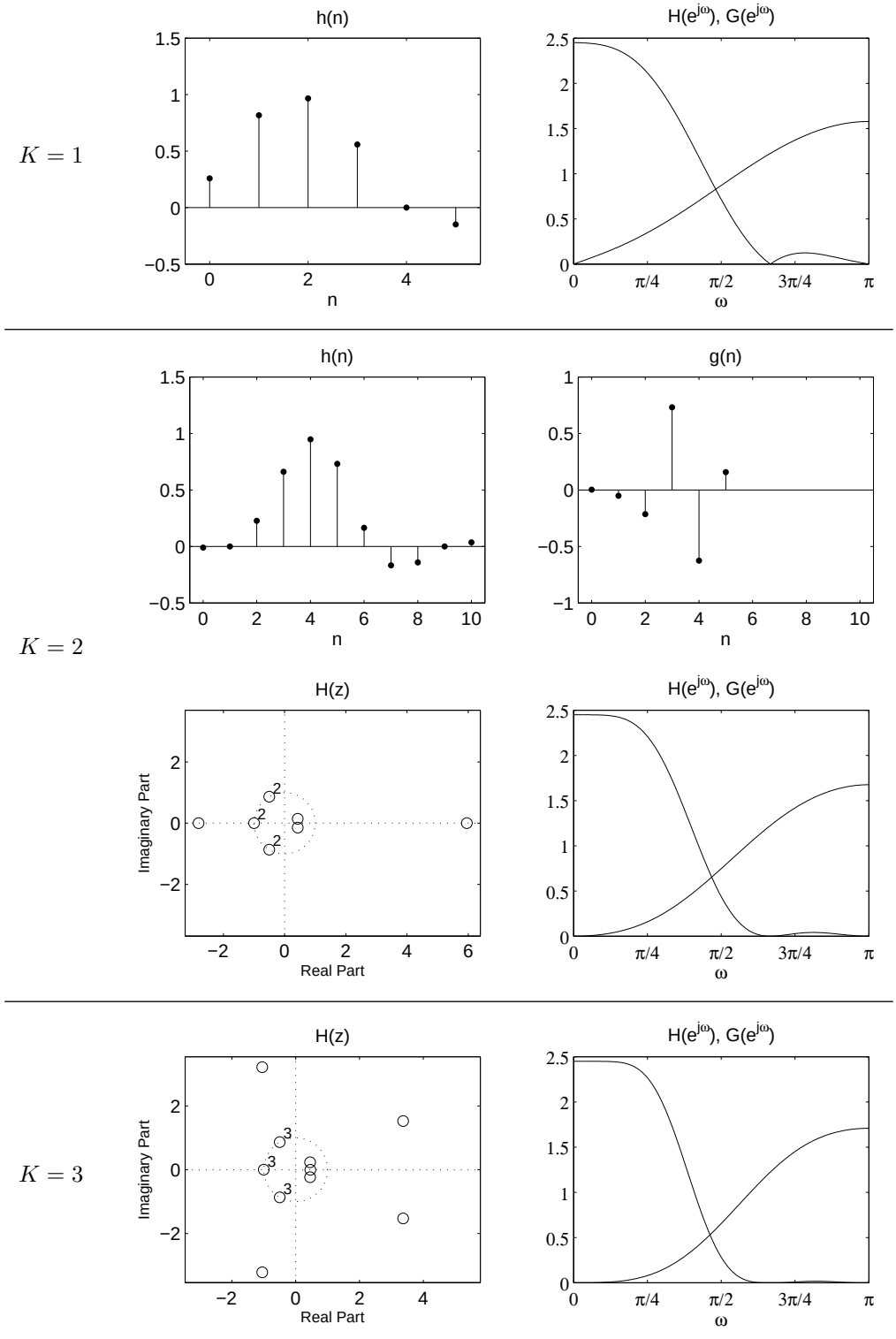

Figure 5. Minimal-length filters with K vanishing moments for orthonormal (2/3) rational filter bank; $K = 1, 2, 3$. The coefficients are tabulated in Table 1.

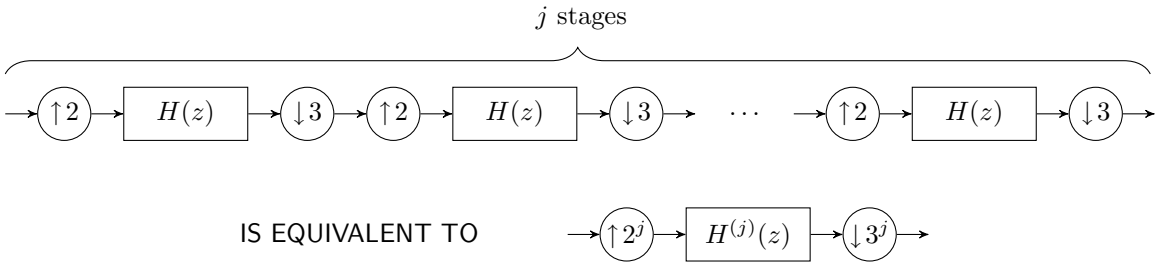

Figure 6. Iterating a rational filter system can be equivalently represented by the systems above. The iterated low-pass filter $H^{(j)}(z)$, defined by the equivalence of the two systems, is given by (23).

For example, $H^{(3)}(z) = H(z^4)\,H(z^6)\,H(z^9)$. For the minimal-length filters with K vanishing moments tabulated in Table 1, the iterated low-pass filter $H^{(j)}(z)$ is illustrated in Fig. 7 (for $K = 1, 3$).

An important difference from the dyadic case arises because of the upsampler. Instead of a single filter, we now see that the input is fed into 2^j different filters and the final output is formed by arranging the samples from the outputs of each of these filters. If we ask that all of these filters be legitimate low-pass filters, then $H(z)$ should have factors[5,8] of the form $(1 + z^{-1} + z^{-2})$. In this subsection we investigate the consequences of these factors. In particular, we show that orthonormality combined with the zeros of $H(z)$ at $z = \{W, W^2\}$ imply that $H(z)$ has the same number of zeros at $z = -1$. Using this fact, we further show that the high-pass filter $G(z)$ has the same number of zeros at $z = 1$. Taken together, this means that, similarly as in the dyadic case, if a rational orthonormal system has K vanishing moments, then the low-pass filter preserves discrete-time polynomial signals of degree $K - 1$, and the high-pass filter eliminates polynomial signals of degree $K - 1$. We start with the zeros of $H(z)$ at $z = -1$.

Multiplying the first row and the second column of the first and second matrix in (10) gives us,

$$H(z^{-1})H(-z) + H(z^{-1}W)H(-zW^2) + H(z^{-1}W^2)H(-zW) = 0. \tag{24}$$

Rewriting we have,

$$H(z^{-1})H(-z) = -H(z^{-1}W)H(-zW^2) - H(z^{-1}W^2)H(-zW). \tag{25}$$

Now if $(z^2 + z + 1)^K$ is a factor of $H(z)$, we can write,

$$H(z) = (z^2 + z + 1)^K C(z), \tag{26}$$

which implies,

$$H(z) = (z - W)^K Q_1(z), \tag{27}$$

and

$$H(z) = (z - W^2)^K Q_2(z), \tag{28}$$

for some finite order Laurent polynomials $C(z)$, $Q_1(z)$ and $Q_2(z)$. From (27), we obtain,

$$H(-zW) = (-zW - W)^K Q_1(z) = (-W)^K (z + 1)^K Q_1(z), \tag{29}$$

and from (28) we obtain,

$$H(-zW^2) = (-zW^2 - W^2)^K Q_2(z) = (-W^2)^K (z + 1)^K Q_2(z). \tag{30}$$

Now using (29) and (30), (25) can be written as,

$$H(z^{-1})H(-z) = -H(z^{-1}W)(-W^2)^K (z + 1)^K Q_2(z) - H(z^{-1}W^2)(-W)^K (z + 1)^K Q_1(z) \tag{31}$$

$$= (z + 1)^K P(z) \tag{32}$$

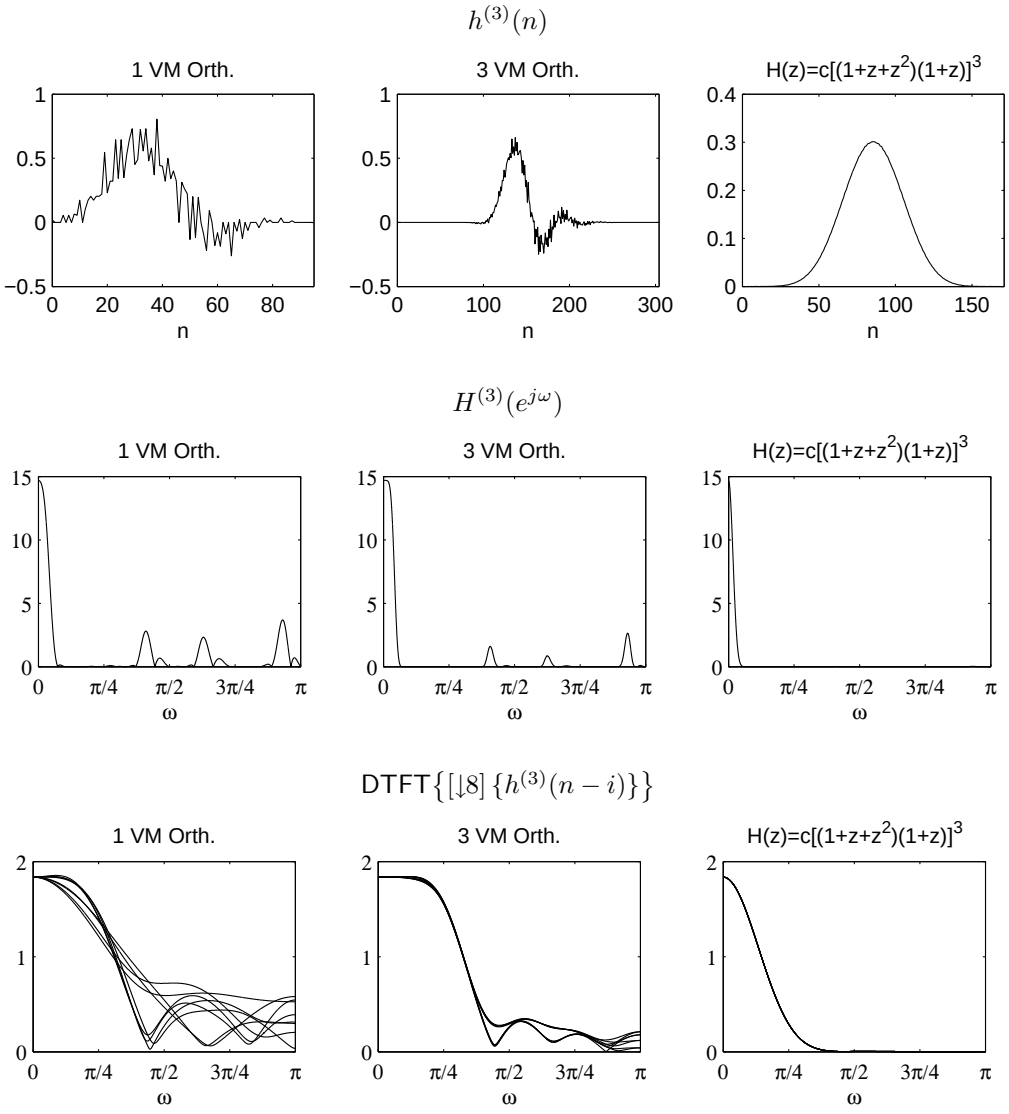

Figure 7. The iterated low-pass filter $H^{(3)}(z)$ for: a minimal-length rational orthonormal DWT with 1 vanishing moment (left), 2 vanishing moments (center), and the rational tight-frame DWT (right) from Sect. 3.1. Top panel: impulse response $h^{(3)}(n)$. Center panel: frequency response $|H^{(3)}(e^{j\omega})|$. Lower panel: frequency responses of the 2^3 polyphase components of $H^{(3)}(z)$.

for some finite order polynomial $P(z)$. If we assume that $H(1) \neq 0$, we see that the term $(z+1)^K$ cannot be a factor of $H(-z)$. Thus we conclude,

$$H(z) = (z^{-1}+1)^K Q(z). \tag{33}$$

To see $H(1) \neq 0$, consider the following equation (row1 $\times$ column1 in (10)):

$$\frac{1}{6}\big(H(z)H(z^{-1}) + H(zW)H(z^{-1}W^2) + H(zW^2)H(z^{-1}W)\big) = 1, \tag{34}$$

equivalently,

$$|H^f(\omega)|^2 + |H^f(\omega - 2\pi/3)|^2 + |H^f(\omega - 4\pi/3)|^2 = 6, \quad \text{with } H^f(\omega) := H(e^{j\omega}). \tag{35}$$

Putting $z = 1$ (equivalently $\omega = 0$) and noting that $H(W) = H(W^2) = 0$, we see that $H(1) = \pm\sqrt{6}$.

Now we look at the zeros of $G(z)$ at $z = 1$. Consider (34) again. Now put $z = -1$. Noting that $H(-1) = 0$, we get $H(-W)H(-W^2) = 3$. Putting $z = W$ in (6), we obtain $G(W)G(W^2) = 3/2$, hence, $G(W) \neq 0$, $G(W^2) \neq 0$. Consider (7). Rewriting this, using the facts derived above,

$$2G(z^2W)G(z^{-2}) = -H(zW^2)H(z^{-1}) - H(-zW^2)H(-z^{-1}) \tag{36}$$

$$= (z-1)^K P_1(z)\, H(z^{-1}) + H(-zW^2)\,(z-1)^K P_2(z) \tag{37}$$

$$= (z-1)^K P(z) \tag{38}$$

Since, $G(W) \neq 0$, it follows that the term $(z-1)^K$ should belong to $G(z^{-2})$ (with an additional $(z+1)^K$ term). This proves that $G(z)$ has a zero of order K at $z = 1$.

A final remark may be made regarding the influence of vanishing moments on the filters in Fig. 6. As mentioned previously, the system in Fig. 6 computes the inner product of the discrete-time input signal with 2^j different sub-sequences of $h(n)$ (the 2^j polyphase components of $h^{(j)}(n)$). Ideally, one would like these sequences to be the same (more accurately, related by a corresponding delay term), but this is too restrictive. Instead, we can ask for approximate satisfaction of this delay property. Blu observes[5] that as the number of vanishing moments increase, the sequences converge to more similar functions (or satisfy the approximate shift property better). To illustrate this point, we show in Fig. 7, the iterated low-pass filter $h^{(3)}(n)$ with 1 and 3 vanishing moments. The lower panel of Fig. 7 illustrates the Fourier transform of all eight sub-sequences of $h^{(3)}(n)$. Notice that $h^{(3)}(n)$ is not smooth for the orthonormal solutions. However, increasing the number of vanishing moments makes the 2^j sub-sequences more similar to each other in addition to increasing their smoothness. The left column of Fig. 7 illustrates the iterated low-pass filter and its 8 sub-sequences, for the low-pass filter (45) used for the construction of the tight frame in Section 3.1. For this case, the iterated low-pass filter is smooth and the 8 sub-sequences are indistinguishable.

3. A RATIONAL TIGHT FRAME

In this section, we consider the design of a rational (2/3) wavelet tight frame based on over-sampled filter banks (see Fig. 8). Like some other wavelet tight frames,[18] the overcomplete transform will be approximately shift-invariant and will sample the time-frequency plane more densely than a critically-sampled wavelet transform. The tight frame introduced here is based on the filter bank in Fig. 8, which possesses two additional high-pass channels (G_1 and G_2 in addition to G_0).

As discussed earlier, the design of an orthonormal rational filter bank (with FIR filters) with vanishing moments requires the solution of a number of nonlinear equations. In contrast with the M-band case, the design of the low-pass filter can not be simplified by expressing the design problem in terms of auto-correlation sequences. However, for the tight frame, the constraints the low-pass filter must satisfy are significantly relaxed. The high-pass filters that complement the low-pass filter (so as to 'complete' the filter bank) can be obtained via polynomial matrix spectral factorization, for which many algorithms are available.

Consider the system in Fig. 8, where the filters $H_0(z)$ and $H_1(z)$ are related to $H(z)$ by (11). Given $H_0(z)$ and $H_1(z)$, our aim is to find $G_i(z)$ so that the resulting filter bank forms a tight frame. Consider the polyphase decompositions of the filters. For $H_0(z)$, this is:

$$H_0(z) = H_{00}(z^3) + z^{-1}H_{01}(z^3) + z^{-2}H_{02}(z^3). \tag{39}$$

Suppose similar notation is used to denote the polyphase components of the remaining filters. The FB is a tight frame iff

$$\begin{bmatrix}\mathbf{H}(z) & \mathbf{G}(z)\end{bmatrix}\begin{bmatrix}\mathbf{H}^T(z^{-1}) \\ \mathbf{G}^T(z^{-1})\end{bmatrix} = \mathbf{I} \tag{40}$$

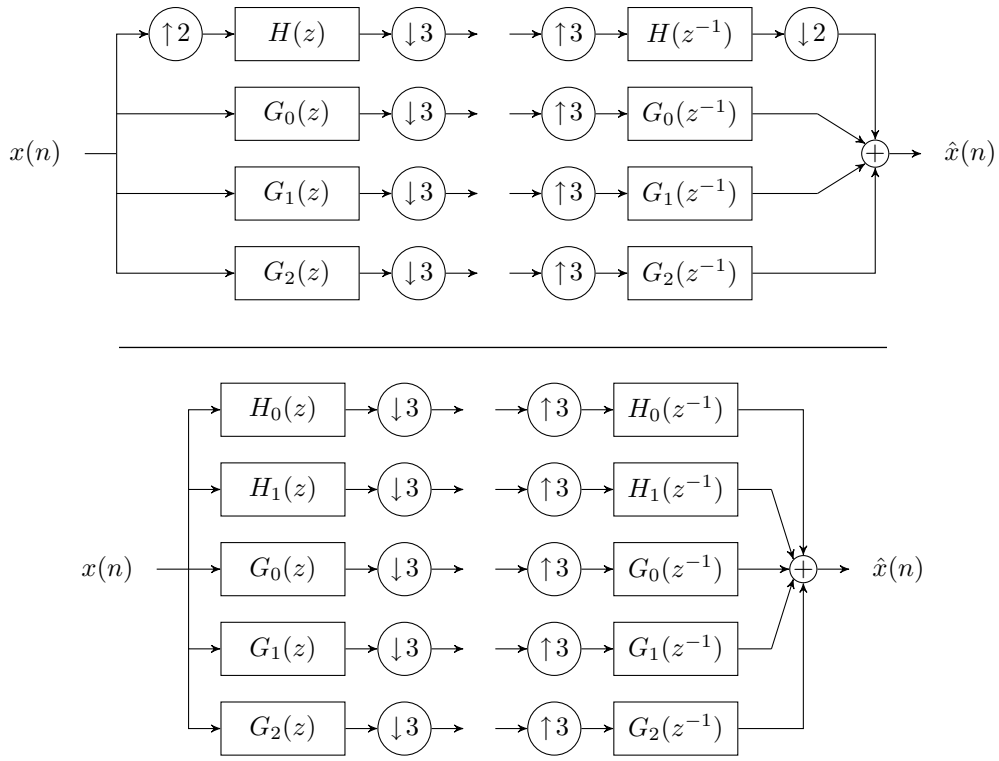

Figure 8. An over-sampled filter bank for implementing a rational wavelet tight frame, and an equivalent system.

where

$$\mathbf{H}(z) = \begin{bmatrix} H_{00}(z) & H_{10}(z) \\ H_{01}(z) & H_{11}(z) \\ H_{02}(z) & H_{12}(z) \end{bmatrix}, \quad \mathbf{G}(z) = \begin{bmatrix} G_{00}(z) & G_{10}(z) & G_{20}(z) \\ G_{01}(z) & G_{11}(z) & G_{21}(z) \\ G_{02}(z) & G_{12}(z) & G_{22}(z) \end{bmatrix}. \tag{41}$$

From (40), we see that,

$$\mathbf{G}(z)\,\mathbf{G}^T(z^{-1}) = \mathbf{I} - \mathbf{H}(z)\,\mathbf{H}^T(z^{-1}). \tag{42}$$

Thus we can complete the FB to a tight frame iff the matrix $\left(\mathbf{I} - \mathbf{H}(z)\,\mathbf{H}^T(z^{-1})\right)$ is non-negative definite on the unit circle. It turns out that a given low-pass filter can be completed to a tight frame as shown in Fig. 8 provided that

$$3 - \sum_{k=0}^{2} |H_0(e^{j(\omega+2k\pi/3)})|^2 \geq 0, \tag{43}$$

and

$$\left(3 - \sum_{k=0}^{2} |H_0(e^{j(\omega+2k\pi/3)})|^2\right)\left(3 - \sum_{k=0}^{2} |H_1(e^{j(\omega+2k\pi/3)})|^2\right) - \left|\sum_{k=0}^{2} H_0(e^{j(\omega+2k\pi/3)}) H_1^*(e^{j(\omega+2k\pi/3)})\right|^2 \geq 0. \tag{44}$$

Notice that if the filters $H_i(z)$ were part of an orthonormal FB, then these equations would hold with equality. Intuitively, the equations say that, the filters should be far enough from being unit energy sequences so that they can be completed so as to eliminate their currently non-zero inner product.

Table 2. The high-pass filters g_i completing the low-pass filter (45) to a rational (2/3) tight frame. The frequency responses $|H^f(\omega)|$ and $|G_i^f(\omega)|$ are also illustrated. Note that the high-pass filters have approximately the same frequency response magnitude. The filters are illustrated in Fig. 9.

n	$g_0(n)$	$g_1(n)$	$g_2(n)$
0	0.64917778505741	0	0
1	-0.48262654366226	0.63770868747435	0
2	-0.15059130119969	-0.46687803212812	0.64520631583316
3	-0.01477135217528	-0.14815175304968	-0.49098922627425
4	-0.00118858802016	-0.02267890229656	-0.13149490989732
5	0	0	-0.02152627546889
6	0	0	-0.00119590419272

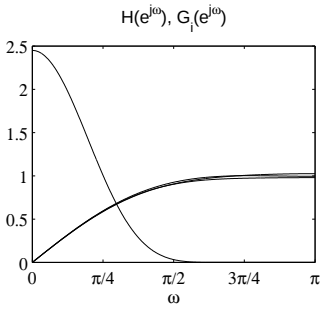

The problem then is to find the 'square root' of $\left(\mathbf{I} - \mathbf{H}(z)\,\mathbf{H}^T(z^{-1})\right)$. As mentioned in the introduction, there are numerous methods to perform this task. We used the *symmetric factor extraction* method described in Ref. 21 (also see Section 2.1 in Ref. 22 and the references therein for a slightly different version of the method). The first step is the computation of the determinant of the matrix and the selection of a subset of its roots (as if one were performing univariate spectral factorization via polynomial root finding). The next step reduces the matrix to a unimodular matrix using structured symmetric factors. Then, this unimodular matrix is further reduced to a constant non-negative definite symmetric matrix. Finally factoring the constant matrix, two factors are obtained as desired. This method allows one to choose the zeros of each factor without any minimum- or maximum-phase restriction, unlike other methods.[22]

3.1 Example

We set the symmetric low-pass filter with 3 zeros at $z = \{W, W^2, -1\}$, normalized so that $H(1) = \sqrt{6}$, i.e.,

$$H(z) = \frac{\sqrt{6}}{6^3}\left[(1 + z + z^2)(1 + z)\right]^3. \tag{45}$$

The frequency response is shown in Table 2. Figure 7 (right column) illustrates the iterated low-pass filter $h^{(3)}(n)$; it is visibly smoother that the iterated low-pass filters of the orthonormal case.

To check whether this low-pass filter can be completed to a tight frame, we evaluate (43) and (44) on the unit circle, using the polyphase components as defined in (11). These turn out to be nonnegative, so this low-pass filter allows a tight frame to be formed. Next, we form the matrix $\mathbf{H}(z)$ using the polyphase components as defined in (11) (notice that $H_{12}(z)$ will not be causal according to this definition). Applying the symmetric factor extraction algorithm in Ref. 21 to perform matrix spectral factorization of $\mathbf{G}(z)\,\mathbf{G}^T(z^{-1})$ in (42) induced by the filter in (45), we obtain $\mathbf{G}(z)$. From $\mathbf{G}(z)$ we obtain the three filters $G_i(z)$, $i = 0, 1, 2$, which, together with the low-pass filter, form a tight frame.

Notice that the factors of the matrix $\mathbf{G}(z)\mathbf{G}^T(z^{-1})$ are not unique. In particular we have,

$$\mathbf{G}(z)\,\mathbf{G}^T(z^{-1}) = \mathbf{G}(z)\,\mathbf{R}(z)\,\mathbf{R}^T(z^{-1})\,\mathbf{G}^T(z^{-1}) \tag{46}$$

where $\mathbf{R}(z)$ is any paraunitary matrix. A possible step then might be to introduce such paraunitary factors so as to improve the frequency responses of $G_i(z)$. Following the concept of the double-density DWT,[29] we might ask that $g_0(n-2) = g_1(n-1) = g_2(n)$, but this is not possible with FIR filters. However, we can approximate this relationship. To gain insight on the extent to which this relationship can be satisfied, consider the PR conditions, this time similar to (6), (7), (8).

$$H_0(z)H_0(z^{-1}) + H_1(z)H_1(z^{-1}) + G_0(z)G_0(z^{-1}) + G_1(z)G_1(z^{-1}) + G_2(z)G_2(z^{-1}) = 3, \tag{47}$$

$$H_0(zW^k)H_0(z^{-1}) + H_1(zW^k)H_1(z^{-1}) + G_0(zW^k)G_0(z^{-1}) + G_1(zW^k)G_1(z^{-1}) + G_2(zW^k)G_2(z^{-1}) = 0, \tag{48}$$

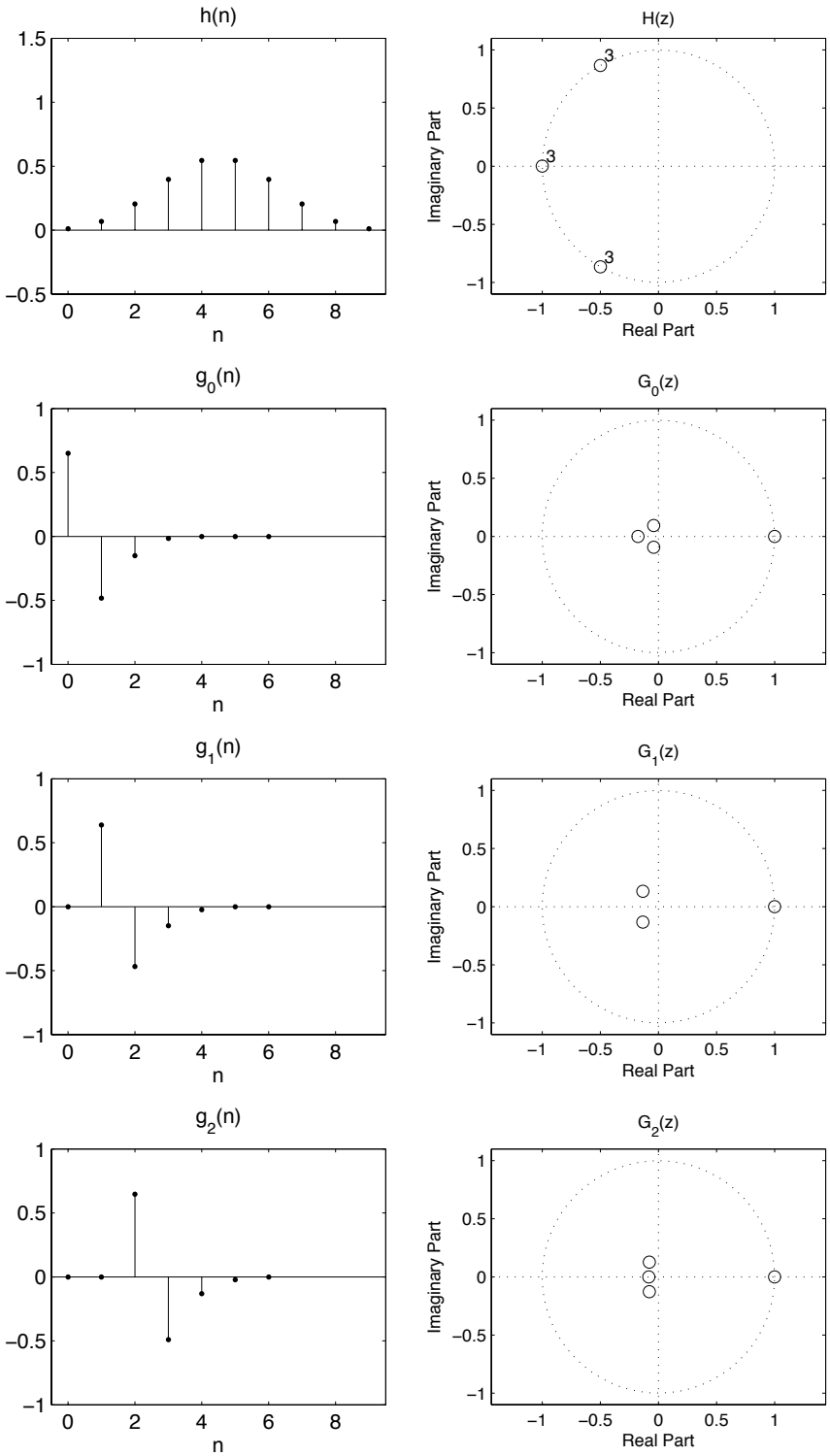

Figure 9. Perfect reconstruction filters for the rational (2/3) overcomplete filter bank of Fig. 8. The impulse responses and zero-diagrams are illustrated. The low-pass filter h is given by (45); the high-pass filters g_i, obtained via polynomial matrix spectral factorization, are tabulated in Table 2. Note that the high-pass filters satisfy (49) and therefore, the transform is approximately shift-invariant.

for $k \in \{1, 2\}$. We would like to find a solution such that,

$$g_0(n-2) \approx g_1(n-1) \approx g_2(n). \tag{49}$$

But this implies

$$G_0(zW^k)\, G_0(z^{-1}) + G_1(zW^k)\, G_1(z^{-1}) + G_2(zW^k)\, G_2(z^{-1}) \approx 0, \tag{50}$$

which in turn requires, from (48) that

$$H_0(zW^k)\, H_0(z^{-1}) + H_1(zW^k)\, H_1(z^{-1}) \approx 0. \tag{51}$$

Provided that this is satisfied, if we write,

$$G(z)\, G(z^{-1}) = 1 - \frac{1}{3}\left[H_0(z)\, H_0(z^{-1}) - H_1(z)\, H_1(z^{-1})\right], \tag{52}$$

it follows that $G_i(z) \approx z^{-i}\, G_0(z)$ is an eligible solution.

Turning back to our example, it turns out that (45) satisfies (51). Therefore, performing rotations similarly as in Ref. 29, we are able to obtain high-pass filters satisfying (49). The resulting filters are tabulated in Table 2 and illustrated in Fig. 9. The frequency decomposition provided by the rational tight frame designed here is illustrated in the lower panel of Fig. 2 — the stop-bands are free of the ripples that are present in the orthonormal solution. Note that the low-pass filter (45) used here is such that (a) the rational wavelet transform has only one vanishing moment, and (b) the passbands of the band-pass filters (illustrated in Fig. 2) have a lower Q-factor compared to the orthonormal (2/3) rational transform.

4. CONCLUSION

We investigated the filter design problem for orthonormal rational FBs. Using Gröbner basis methods, we obtained minimal-length solutions for the orthonormal (2/3) rational filter bank with K vanishing moments, with $K = 1, 2, 3$. We also considered the design of rational tight frames, which sample the time-frequency plane more densely, can be approximately shift invariant, and provide additional degrees of freedom for the design. For a given low-pass filter, we presented the necessary conditions for completion, described the completion using matrix spectral factorization, and demonstrated the design procedure in an example.

REFERENCES

1. F. Argenti and E. Del Re. Rational sampling filter banks based on IIR filters. *IEEE Trans. Signal Processing*, 46(12):3403–3408, December 1998.
2. P. Auscher. Wavelet bases for $L^2(R)$ with rational dilation factor. In M. B. Ruskai et al., editor, *Wavelets and Their Applications*. Jones and Barlett, Boston, 1992.
3. A. Baussard, F. Nicolier, and F. Truchetet. Rational multiresolution analysis and fast wavelet transform: application to wavelet shrinkage denoising. *Signal Processing*, 84(10):1735–1747, October 2004.
4. P. Blanc, T. Blu, T. Ranchin, L. Wald, and R. Aloisi. Using iterated rational filter banks within the ARSIS concept for producing 10 m Landsat multispectral images. *International Journal of Remote Sensing*, 19(12):2331–2343, August 1998.
5. T. Blu. Iterated filter banks with rational rate changes – connection with discrete wavelet transforms. *IEEE Trans. Signal Processing*, 41(12):3232–3244, December 1993.
6. T. Blu. An iterated rational filter bank for audio coding. In *Proc. IEEE Int. Symposium on Time-frequency and Time-scale Analysis*, 1996.
7. T. Blu. A new design algorithm for two-band orthonormal rational filter banks and orthonormal rational wavelets. *IEEE Trans. Signal Processing*, 46(6):1494–1504, June 1998.
8. T. Blu and O. Rioul. Wavelet regularity of iterated filter banks with rational sampling changes. In *Proc. IEEE Int. Conf. on Acoustics, Speech and Signal Proc. (ICASSP)*, 1993.

9. G. F. Choueiter and J. R. Glass. An implementation of rational wavelets and filter design for phonetic classification. *IEEE Trans. Audio, Speech and Lang. Proc.*, 15(3):939–948, March 2007.
10. C. K. Chui, W. He, and J. Stöckler. Compactly supported tight and sibling frames with maximum vanishing moments. *Appl. Comput. Harmon. Anal.*, 13(3):224–262, November 2002.
11. D. A. Cox, J. B. Little, and D. O'Shea. *Ideals, Varieties and Algorithms*. Springer, 1996.
12. I. Daubechies. *Ten Lectures on Wavelets*. SIAM, 1992.
13. F. C. C. B. Diniz, I. Koethe, S. L. Netto, and L. W. P. Biscainho. High-selectivity filter banks for spectral analysis of music signals. *EURASIP Journal on Advences in Signal Processing*, 2007:Article ID 94704, 12 pages, 2007. doi:10.1155/2007/94704.
14. G. Evangelista and S. Cavaliere. Discrete frequency warped wavelets: Theory and applications. *IEEE Trans. Signal Processing*, 46(4):874–885, August 1998.
15. G.-M. Greuel, G. Pfister, and H. Schönemann. SINGULAR 3.0. A Computer Algebra System for Polynomial Computations, Centre for Computer Algebra, University of Kaiserslautern, 2005. `http://www.singular.uni-kl.de`.
16. B. Han and Q. Mo. Splitting a matrix of laurent polynomials with symmetry and its application to symmetric framelet filter banks. *SIAM J. on Matrix Analysis and its Appliations*, 26(1):97–124, 2004.
17. D. P. Hardin, T. A. Hogan, and Q. Sun. The matrix-valued Riesz lemma and local orthonormal bases in shift-invariant spaces,. *Adv. Comput. Math.*, 20(4):367–384, 2004.
18. J. Kovačević and A. Chebira. Life beyond bases: The advent of frames (Part I). *IEEE Signal Proc. Mag.*, 24(4):86–104, July 2007. Part II to appear.
19. J. Kovačević and M. Vetterli. Perfect reconstruction filter banks with rational sampling rate changes. In *Proc. IEEE Int. Conf. on Acoustics, Speech and Signal Proc. (ICASSP)*, 1991.
20. J. Kovačević and M. Vetterli. Perfect reconstruction filter banks with rational sampling factors. *IEEE Trans. Signal Processing*, 41(6):2047–2066, June 1993.
21. V. Kučera. *Analysis and Design of Discrete Linear Control Systems*. Prentice Hall, 1991.
22. V. Kučera. Factorization of rational spectral matrices: A survey of methods. In *Proc. IEE Int. Conf. on Control*, 1991.
23. M. Lang and B.-C. Frenzel. Polynomial root finding. *IEEE Signal Processing Letters*, 1(10):141–143, October 1994.
24. J. Lebrun and I. Selesnick. Gröbner bases and wavelet design. *Journal of Symbolic Computing*, 37(2):227–259, February 2004.
25. A. S. Mehr and T. Chen. Design of nonuniform multirate filter banks by semidefinite programming. *IEEE Trans. Circuits Syst. II*, 47(11):1311–1314, November 2000.
26. K. Nayebi, T. P. Barnwell III, and M. J. T. Smith. The design of perfect reconstruction filter banks with rational sampling factors. In *Proc. IEEE Int. Conf. Acoust., Speech and Sig. Proc. (ICASSP)*, 1991.
27. G. Pau, B. Pesquet-Popescu, and G. Piella. Modified M-band synthesis filter bank for fractional scalability of images. *IEEE Signal Processing Letters*, 13(6):345–348, June 2006.
28. J. Princen. The design of nonuniform modulated filterbanks. *IEEE Trans. Signal Processing*, 43(11):2550–2560, November 1995.
29. I. W. Selesnick. The double density DWT. In A. Petrosian and F. G. Meyer, editors, *Wavelets in Signal and Image Analysis: From Theory to Practice*. Kluwer, 2001.
30. P. Steffen, P. N. Heller, R. A. Gopinath, and C. S. Burrus. Theory of regular M-band wavelet bases. *IEEE Trans. Signal Processing*, 41(12):3497–3511, December 1993.
31. P.P. Vaidyanathan. *Multirate Systems and Filter Banks*. Prentice Hall, 1992.
32. S. Wada. Design of nonuniform division multirate fir filter banks. *IEEE Trans. Circuits Syst. II*, 42(2):115–121, February 1995.
33. X. M. Xie, S. C. Chan, and T. I. Yuk. Design of perfect reconstruction nonuniform recombination filter banks with flexible rational sampling factors. *IEEE Trans. Circuits Syst. I*, 52(9):1965–1981, September 2005.
34. D. Youla and N. Kazanjian. Bauer-type factorization of positive matrices and the theory of matrix polynomials orthogonal on the unit circle. *IEEE Trans. Circuits and Syst.*, 25(2):57–69, February 1978.